Zirconium deficit as a tracer of urban sediment accumulation in Sustainable Urban Drainage Systems – Application to the calibration of a filtration model

Damien Tedoldi, Kelsey Flanagan, Ghassan Chebbo, Philippe Branchu, Daniel Pierlot, Marie-Christine Gromaire

Zirconium deficit as a tracer of urban sediment accumulation in Sustainable Urban Drainage Systems – Application to the calibration of a filtration model

Damien TEDOLDI[1,2,*], Kelsey FLANAGAN[1], Ghassan CHEBBO[1,3], Philippe BRANCHU[4], Daniel PIERLOT[2], and Marie-Christine GROMAIRE[1]

[1]LEESU, UMR MA 102, École des Ponts, AgroParisTech, UPEC, UPE, Champs-sur-Marne, 6-8 avenue Blaise Pascal, Cité Descartes, 77455 Marne-la-Vallée Cedex 2, France. damien.tedoldi@enpc.fr, kelsey.flanagan@enpc.fr, ghassan.chebbo@enpc.fr, marie-christine.gromaire@enpc.fr

[2]SEPIA, 53 rue de Turbigo, 75003 Paris, France. dp@sepia-uw.fr

[3]Faculty of Engineering III, Lebanese University, Hadath, Lebanon.

[4]CEREMA, 12 Rue Léon Teisserenc de Bort, 78190 Trappes, France. philippe.branchu@cerema.fr

*Corresponding author

ABSTRACT

Among the processes governing contaminant retention in soil-based *Sustainable Urban Drainage Systems* (SUDS), quantifying the relative contribution of particle settling and filtration requires a tracer of runoff-generated solids. Since zirconium (Zr) is a widely used geochemical invariant in pedological approaches, with few anthropogenic sources, the present investigation aims to assess whether its use may be extended to sediment identification in SUDS. High-resolution horizontal and vertical soil sampling was carried out in 11 infiltration systems, as well as in road-deposited sediment. Following elemental analysis *via* X-ray fluorescence spectrometry, the spatial distribution of both Zr and urban-derived metals could be determined. Zr content in sediment was found to be fairly stable and significantly lower than in soil. In most devices, Zr and metals exhibited "mirror" trends, both horizontally and vertically, *i.e.* a deficit of Zr could be observed in the most contaminated area. This indicated a "dilution-like" mixture of soil and sediment, the fraction of which could be calculated and appraised spatially. The vertical profiles proved the occurrence of bed filtration over 5 to 15 cm, and enabled the calibration of a simple filtration model. The uncertainties associated with the determined filter coefficient were found to be comparable to the other experimental methods – with the additional improvement that the present approach does not require water sampling.

KEYWORDS

Runoff infiltration, Soil, Urban environment, Urban sediment, X-ray fluorescence, Zirconium

1. INTRODUCTION

Stormwater management close to the source, referred to variously as *Low Impact Development* (LID), *Best Management Practices* (BMPs), *Water Sensitive Urban Design* (WSUD), or *Sustainable Urban Drainage Systems* (SUDS), has gained popularity across the world (Fletcher *et al*., 2015), in order to mitigate the adverse effects of urban development and rising levels of impervious cover on the water cycle – namely, increased peak flows and annual volumes of runoff, faster hydrological response of the catchments, reduced infiltration and groundwater recharge (Fletcher *et al*., 2013; Miller *et al*., 2014), along with several qualitative impacts on the receiving water bodies (Hatt et al., 2004; McGrane, 2016). In addition to their widely recognized hydrologic and hydraulic benefits, these systems, and especially soil- or media-based devices, offer interesting perspectives towards the interception of diffuse pollutant fluxes in urban environments (Dierkes *et al*., 2015; Napier *et al*., 2009; Paus *et al*., 2013). On one hand, particle-bound contaminants in runoff are likely to be trapped with suspended solids *via* deposition and filtration, sometimes leading to the progressive formation of a sediment layer at the surface of infiltration systems (El-Mufleh *et al*., 2014; Erickson *et al*., 2013). On the other hand, dissolved species may undergo sorption onto various reactive constituents of the solid matrix (Sposito, 2008; Tedoldi *et al*., 2016). Since several contaminants such as trace metals are present in both dissolved and particulate forms in urban runoff, their accumulation in soil (or filter media) results from a combination of these physical and physico-chemical mechanisms.

Conventional experimental assessments of soil contamination in SUDS, which consist of collecting and analyzing soil samples after a known operation time, provide an overall and "time-integrated" vision of these retention processes (Kluge and Wessolek, 2012; Tedoldi *et al*., 2017a). However, they do not enable to differentiate between the relative contributions of settling/filtration and sorption, especially because runoff-generated solids – hereafter referred to as "sediment" – are not quantified *in the solid phase*.

As discussed by Clark and Pitt (2012), while infiltration practices are often designed according to empirical recommendations, and their treatment performance extrapolated from a limited number of field studies, a better understanding of the retention mechanisms taking place could valuably improve their choice, design and maintenance. Additionally, soil clogging by runoff sediment has often been reported as a major concern in infiltration systems, but it remains difficult to characterize and quantify the state of clogging in a given device, or even to anticipate the occurrence of hydraulic malfunction (Cannavo *et al*., 2018). Finally, if the long-term fate of contaminants in SUDS soil is to be appraised with a modelling approach, it seems necessary to consider the behavior of particle-bound species in addition to solute transport. Although several filtration models are available for this purpose (Logan, 2001), few authors attempted to do so (Li and Davis, 2008a), possibly because of the difficulty to calibrate such models with usual field data (Tedoldi *et al*., 2016). To this end, the vertical distribution of filtered particles – provided it may be accurately determined – may constitute useful calibration data. All these points highlight the interest of identifying a tracer of urban sediment accumulation in SUDS.

The latter should (*i*) be conservative in a pedological acceptation, *i.e.* its content in soil should not be affected by runoff infiltration (neither *via* sorption nor *via* lixiviation), and (*ii*) display an anthropogenic signal different from the local background level in soils. The first point typically prevents the use of heavy metals such as copper or zinc, which are also present in the dissolved form in runoff (their average dissolved fractions reported by Huber *et al*. (2016) in road runoff were 38 and 31%, respectively) and have a strong affinity for the soil constituents (Tedoldi *et al*., 2016).

Due to their very low mobility in soils under almost all environmental conditions, resistance to weathering, and very low availability to plants, elements such as titanium (Ti) and zirconium (Zr) are generally considered as geochemical invariants (Kabata-Pendias, 2011; Schulz, 1965; Shahid *et al*., 2013); hence, they are commonly used as references to calculate enrichment or depletion factors of other elements (Egli and Fitze, 2000; Stockmann *et al*., 2016). However, Ti has been quantified at relatively high levels (> 1 g/kg) in urban road dust (Apeagyei *et al*., 2011), and has numerous anthropogenic sources including paint pigments, car manufacturing, and metallic alloys (Salminen, 2005). Conversely, the anthropogenic sources of Zr are quite limited – nuclear fallout and ceramic dust being the most frequently cited ones (Salminen, 2005; Shahid *et al*., 2013) –, as a result of which the contents in road dust were found to be much lower (~200 mg/kg) (Apeagyei *et al*., 2011). It was observed that the presence of a dense urban area did not significantly impact Zr concentrations in both water and sediment from an urban stream (Mohiuddin *et al*., 2010). Furthermore, the lithogenic sources of Zr and its consequent abundance in most soils enable a systematic quantification with analytical methods such as X-ray fluorescence (Kabata-Pendias, 2011), thus providing the opportunity to extend the number of analyses and to achieve a finer description of its spatial variability.

Therefore, the objective of the present work is to assess the potential use of Zr as an unequivocal tracer of sediment accumulation in SUDS, and to illustrate a possible application with the calibration of a simple filtration model. The approach relies on high-resolution horizontal and vertical soil sampling from 11 infiltration systems, and subsequent analysis of both Zr and three typical urban- and traffic-derived trace metals (Cu, Pb, and Zn). The latter, which are ubiquitous in stormwater runoff (Göbel *et al*., 2007; Huber *et al*., 2016), will be considered as a signature of runoff-induced contamination, and used as a comparison basis.

2. MATERIALS & METHODS

2.1 Description of the study sites

Four small sized infiltration basins, five swales, and two grassed filter strips (Table 1), located in the Paris region (Figure 1), were selected for their contrasting hydraulic configurations, soil types, watersheds, and runoff contamination potentials (Tedoldi *et al*., 2017a). Inflow of water into the infiltration systems consists of either an inlet pipe (*Dourdan*, *Greffiere*, *Alfortville*, *Vaucresson*), or surface runoff directly flowing from

the pavement, with a localized (*Sausset2*) or diffuse inflow (*Sausset1*, *Chanteraines*, *Vitry*, *Compans1*, *Compans2*, *Compans3*). In some devices, superficial outflow is possible in addition to infiltration: in the case of *Dourdan*, *Chanteraines*, and *Vitry*, this occurs when water ponding exceeds a given level, whereas in *Compans1* and *2*, water storage is supposedly achieved in a downstream longitudinal ditch; however, previous studies have shown that most water infiltrates in the roadside filter strips (Flanagan *et al*., 2017). *Compans3* is equipped with a V notch weir.

In *Chanteraines*, *Vitry*, *Compans1* and *2*, the surface soil displays a 5 to 15% slope perpendicular to the pavement; *Alfortville* and *Compans3* have a V-shaped transversal section; the rest of the facilities were constructed with flat bottoms and sharp embankments. *Chanteraines*, *Vitry*, and *Compans2* were excavated and backfilled with topsoil from another site during construction, as were *Compans1* and *3* with an engineered filter media (mixture of calcareous sand and loamy soil). The other systems were implemented upon the preexisting soil.

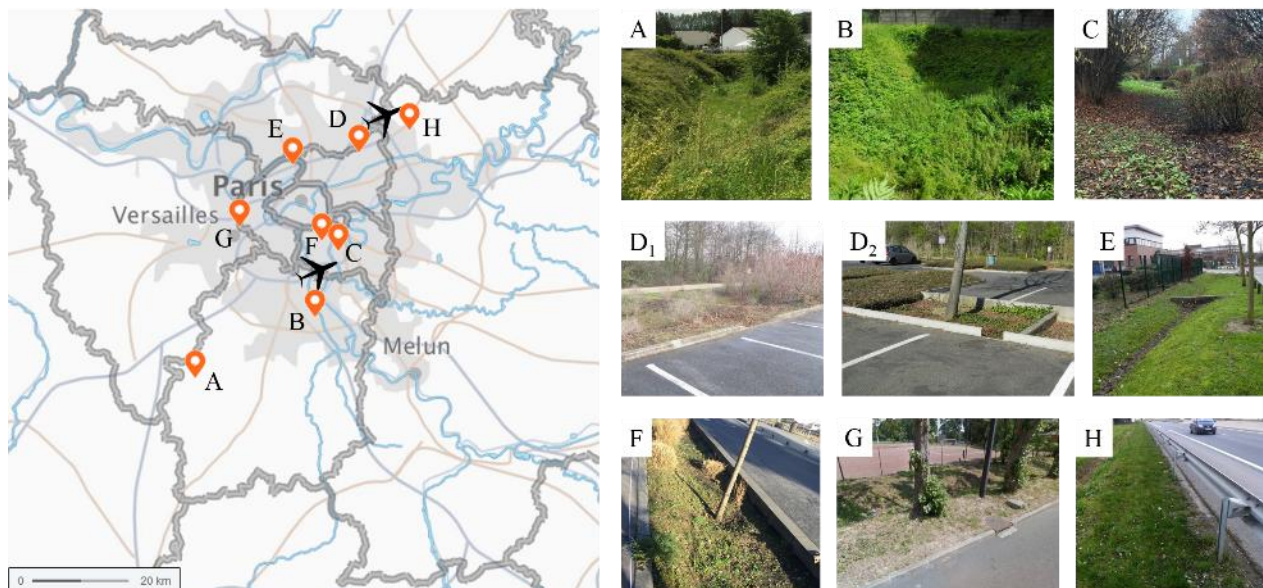**Table 1** – Main characteristics of the investigated infiltration facilities.

Site name	*Dourdan*	*Greffiere*	*Alfortville*	*Sausset1*	*Sausset2*
Type of device	Infiltration-retention basin	Infiltration basin	Infiltration basin	Infiltration basin	Small swale
Catchment characteristics	Two-lane departmental road (4900 veh/day) + car parking lot	Residential catchment: houses with tile roofs and metallic elements	Industrial activities + service roads + logistics area (high truck traffic)	Car parking lot (210 veh/day)	Car parking lot (210 veh/day)
Active area of the catchment	7000 m^2	3000 m^2	20000 m^2	400 m^2	160 m^2
Device area[‡]	120 m^2	65 m^2	130 m^2	68 m^2	10 m^2
Inflow of water	Pipe (Ø600 mm) followed by a concrete apron	Pipe (Ø300 mm)	Pipe (Ø800 mm)	Surface runoff, large opening (90 cm)	Surface runoff, small opening (15 cm)
Superficial outlet	Elevated pipe (30 cm above the ground)	None	None	None	None
Operating time	> 20 years	15 years	16 years	14 years	14 years
Soil texture (0-10 cm)	Sandy loam	Sandy clay loam	Clay loam	Silt loam	Silt loam
Vegetation	Spontaneous vegetation	Spontaneous vegetation	Spontaneous vegetation	Shrubs and grass	Herbaceous plants

Table 1 (*continued*) – Main characteristics of the investigated infiltration facilities.

Chanteraines	*Vitry*	*Vaucresson*	*Compans1*	*Compans2*	*Compans3*
Swale	Swale	Swale	Filter strip	Filter strip	Swale
Service road (< 1500 veh/day) + small car parking lot	T-junction within an industrial catchment (high truck traffic)	Two-lane departmental road (4000 veh/day)	Highway (11000 veh/day in each direction) in the vicinity of an industrial area	Highway (11000 veh/day in each direction) in the vicinity of an industrial area	Highway (11000 veh/day in each direction) in the vicinity of an industrial area
470 m^2	350 m^2	400 m^2	250 m^2	250 m^2	330 m^2
54 m^2	19 m^2	12 m^2	33 m^2	33 m^2	23 m^2
Surface runoff, diffuse inflow	Surface runoff, multiple lateral openings	Pipe (Ø200 mm)	Surface runoff, diffuse inflow	Surface runoff, diffuse inflow	Surface runoff, diffuse inflow
Elevated pipe (25 cm above the ground)	Elevated pipe (25 cm above the ground)	None	Longitudinal ditch	Longitudinal ditch	V notch weir
10 years	10 years	> 25 years	3 years	3 years	1 year
Sandy loam[⋆]	Loam[⋆]	Clay loam	Sandy loam[⋆]	Silt loam[⋆]	Sandy loam[⋆]
Grass	Herbaceous plants	Spontaneous vegetation	Grass	Grass	Grass

‡The given value corresponds to the area of the sampled section during the initial field investigations (*cf.* Section 2.2).
⋆Amended topsoil (different from the preexisting soil).

Figure 1 – Location and photographs of the study sites: A) *Dourdan*, B) *Greffiere*, C) *Alfortville*, D$_1$) *Sausset1*, D$_2$) *Sausset2*, E) *Chanteraines*, F) *Vitry*, G) *Vaucresson*, H) *Compans*.

2.2 Sampling procedure

The field investigations were undertaken in two phases between April 2015 and May 2016, so as to consecutively obtain the distribution of the chemical species of interest at the surface and along vertical profiles (Figure 2). Firstly, a systematic sampling of the surface horizon was carried out using a rectangular grid, with a mesh size adapted to each site so as to meet the strictest of these two criteria: (*i*) collect ≥ 20 samples per device, and (*ii*) collect ≥ 35 samples/100 m^2. At each node, the vegetation was removed if present, then ~50 g of surface soil (upper 2-3 cm) was composited from ≥ 4 subsamples surrounding the sampling location, using a stainless steel trowel which was subsequently cleaned and rinsed twice with ultrapure water. Altogether, nearly 550 soil samples were collected during this phase, all of which were conserved in individual high-density polyethylene bottles prior to analysis (Section 2.3).

This first characterization enabled the identification of the most and the least contaminated areas of each facility, defined as the domains where metal contents were respectively (*i*) higher than the 9th decile, and (*ii*) lower than the 1st decile of the measurements in the site; the latter was considered as a "reference zone" (Figure 2). In each area, 4 core samples were collected with a stainless steel gouge auger, then the upper 30 cm were subdivided into 6 depth sections, with a higher resolution near the surface (2.5-cm-thick segments). For each depth, a composite sample (~250 g) was formed from the 4 corresponding subsamples. This step could not be completed in *Vaucresson* because of maintenance work undertaken by the municipality, which destructured the soil of the swale after the initial sampling campaign. In *Compans1* and *2*, due to the presence of the road sub-base, the soil thickness in the most contaminated zone was insufficient to perform corings. A different methodology was thus applied, which consisted of collecting soil cores at several distances from the road (30, 70, 120, and 180 cm), the thickness of which depended on the depth of the sub-base (7-30 cm); each core was then subdivided into 2 or 3 depth sections, and the samples were analyzed separately.

Whenever present, additional samples of raw sediment were collected on the nearby road pavement (Figure S1); such deposits could not be found in the immediate vicinity of *Alfortville* and *Sausset*.

2.3 Sample preparation and analysis

All samples (soil and sediment) were pre-treated according to the international standard on the preservation and pre-treatment of solid samples for the analysis of non-volatile species (ISO 11464, 2006), *i.e.* oven-dried at 40°C for 7 days, ground with a pestle, then passed through a 2-mm nylon sieve. Elemental analysis was performed *via* X-ray fluorescence (XRF) spectrometry (*Thermo Scientific*, Portable Niton™ analyzer XL3t). 5 to 6 homogenized subsamples were poured as loose powder into polyethylene cells with a thin transparent film at the bottom, and analyzed independently. The elements of interest were copper, lead, zinc, and zirconium. The analysis time was set to 60 s per beam in a standard soil mode. The repeatability of the measurements was checked by calculating the relative standard deviation (RSD) of the 5-6 values for each element, which was always < 10%, with an average of 4-5% for metals and 3% for Zr; similar RSD were

found for soil and sediment samples. Each sample was then assigned its average content of Cu, Pb, Zn, and Zr, calculated from the 5-6 measurements.

In the following developments, unless otherwise specified, soil concentrations will be given in milligrams per kilogram of dry matter (DM). The limits of quantification are sample-dependent, as they vary according to the signal received by the analyzer, but they were always $\leq$ 20, 10, and 30 mg/kg DM for Cu, Pb, and Zn, respectively, and $\leq$ 10 mg/kg DM for Zr.

Since XRF is a non-conventional practice for elemental analysis, a comparison with two reference approaches was carried out – *i.e.* ICP-based analyses on acid-digested samples (for Cu, Pb, Zn) and NIST soil standards (for all elements) – in order to assess the reliability of the XRF-determined contents. The first approach, which has been published in a previous work (Tedoldi *et al*., 2017a), evidenced a satisfactory precision for Cu (mean deviation of 7% from the reference contents) and Zn (14%), and showed that Pb contents were consistently underestimated by 16 mg/kg (which in proportion is higher than for the other two metals – up to 80% – because Pb contamination is lower) when considering XRF measurements. The second approach displayed relative errors ranging from -12 to 5% for Cu, -7 to 16% for Zn, -35 to -13% for Pb, and 4 to 18% for Zr (negative values indicate an underestimation of the certified contents). Besides, it should be added that this analytical technique has been widely used for the quantification of Zr levels, *e.g.* for the construction of the Geochemical Atlas of Europe (Salminen, 2005), and the analysis of road dust (Apeagyei *et al*., 2011).

Additionally, a fraction (~10 g) of each sample was calcined at 550°C for 6 hours, so as to determine its volatile matter content from mass difference.

2.4 Data handling

Surface contents were interpolated so as to generate cartographies of trace metals and zirconium, using a 10 cm × 10 cm interpolation grid covering the whole sampled area of each device. In the subsequent results and discussion, the mention of the SUDS "*surface soil*" will refer to the layer sampled during this first step, *i.e.* the upper 2-3 cm. The data acquired during the second phase were represented as vertical profiles, *i.e.* the evolution of the metal and Zr contents with increasing depth, in the two sampled zones (Figure 2). For *Compans1* and *2*, instead of concentration profiles, the values were interpolated along the sampled transversal sections; the z-coordinate which was associated to each segment corresponded to its *average depth*, assuming that concentrations varied linearly within vertical samples – thus leading to a correspondence between the measured contents and the midpoint of the segments.

As some variables could not be considered as normally distributed, statistical correlations were assessed *via* Spearman's rank correlation coefficient ρ, and the associated non-parametric test of significance. ρ_{XY} corresponds to the Pearson's correlation coefficient between the rank values of the two variables X and Y.

Figure 2 – Schematic representation of the two-step methodology for soil sampling and analysis.
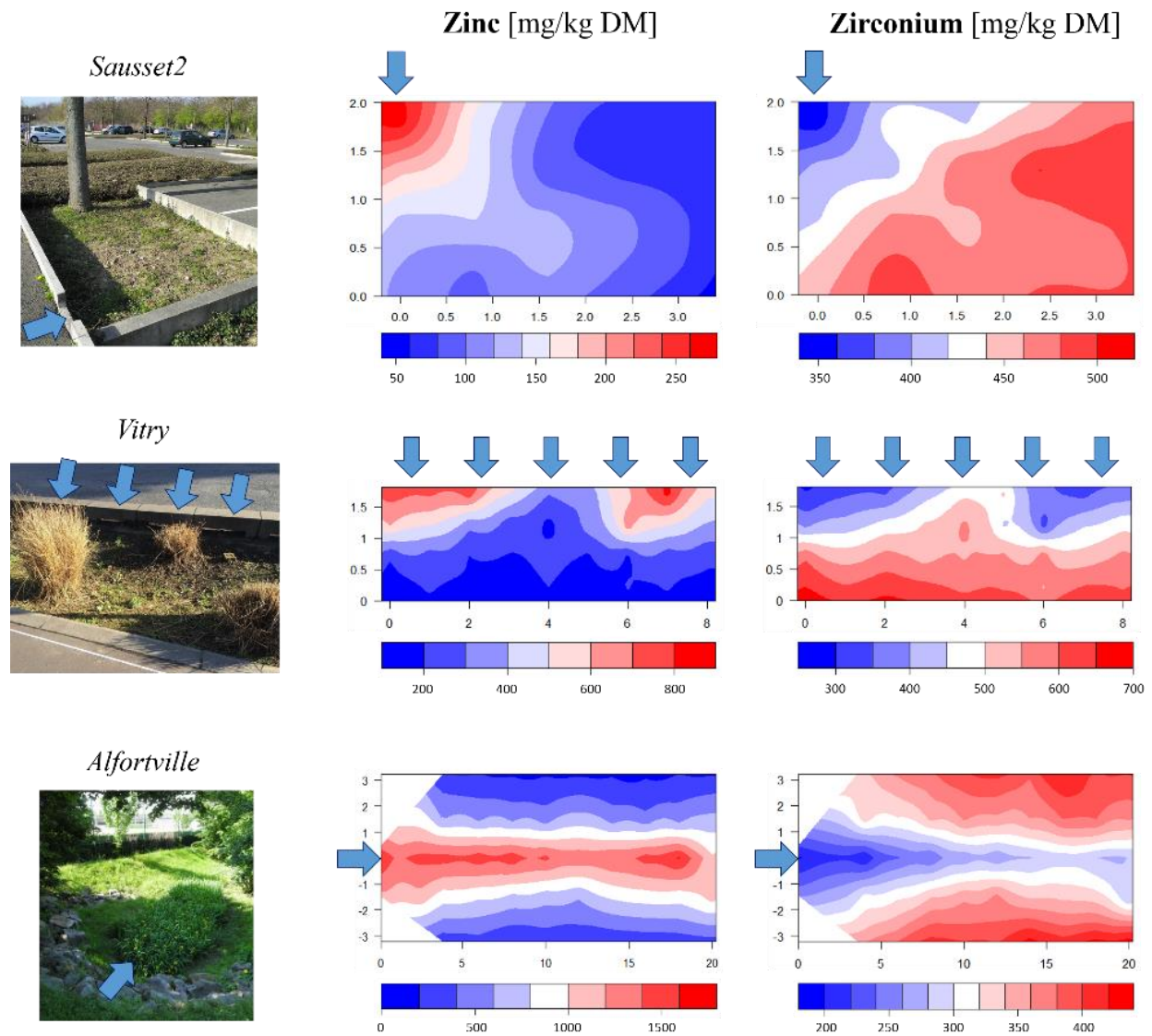
3. RESULTS

3.1 Spatial distribution of metals and Zr in the surface soil

Whatever the study site, Cu, Pb, and Zn exhibited similar distributions in the surface soil, which were characterized by a significant buildup near the inflow area, followed by a marked decrease in concentrations with increasing distance. Figures 3 and 4 present the results obtained for Zn, while the distributions of the other two metals are presented as *supplementary data* (Figure S2). The difference in metal contents between the most and the least contaminated areas of each device is illustrated on Figure S3. Zn and Cu were strongly correlated with $\rho \geq 0.86$ (Table S1), which was statistically significant (*p*-value $< 10^{-10}$). This observation was also applicable for the Zn-Pb correlations in most sites ($\rho \geq 0.84$); lower – albeit significant – correlations were found in *Sausset1*, *Sausset2* and *Chanteraines*, where Pb contamination was inferior (because of limited loads from the watersheds) and the contents rapidly fell within the natural variability of the geochemical background. As a result, zinc could be considered representative of the metal's behavior in the topsoil of the devices, and will be focused on in the subsequent developments.
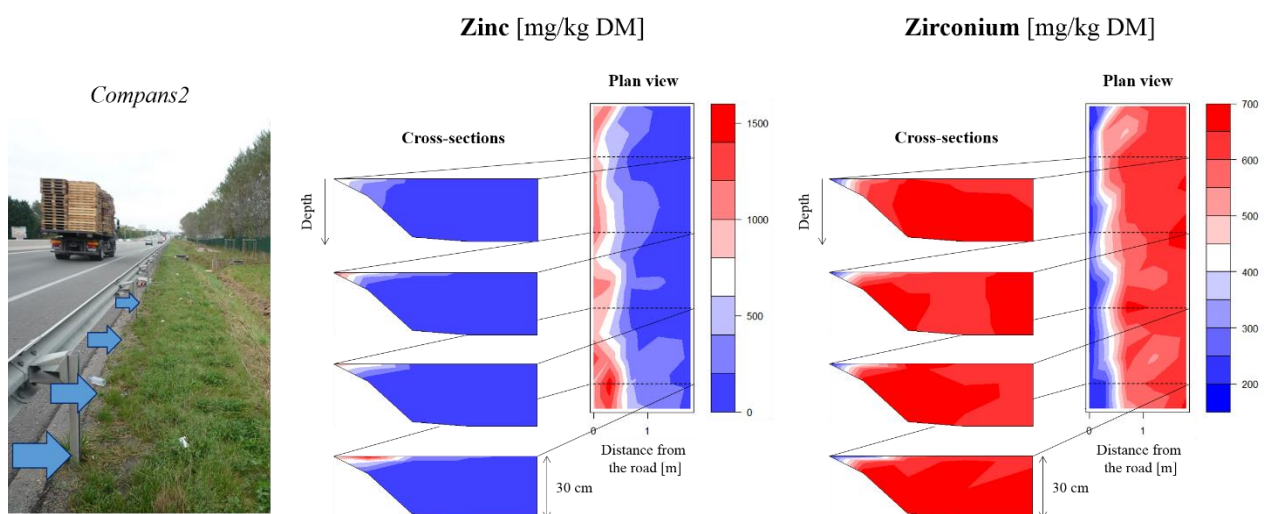
This spatial distribution, the origins and implications of which have been thoroughly discussed elsewhere (Tedoldi *et al.*, 2017a), constituted a precise, "time-integrated" signature of both non-uniform infiltration fluxes and settling processes at the surface of each device. In particular, it provided evidence that the area affected by runoff-derived contamination was horizontally localized – with the exception of the *Alfortville* basin (Figure 3), whose atypical behavior was due to the presence of a clay horizon at 25 cm depth, thus preventing the fast infiltration of water near the inlet pipe: hence, the lowest part of the V-shaped basin (located at the coordinate $y = 0$) was almost evenly polluted by trace metals.

Remarkably, Zr commonly showed "mirror" distributions with respect to metals: in other words, a deficit of this element could be observed in the most contaminated zone, with an opposite increasing trend toward the reference zone (Figures 3, 4, and S3). The marked – albeit reverse – similarity between Zr and metal distributions was generally characterized by negative correlations with various levels of significance (Table S1), leading to the following classification:

i. In *Alfortville*, *Sausset1*, *Vitry*, *Compans1*, and *Compans2*, the correlations were significant with $\rho \leq -0.78$ (excluding Pb in *Sausset1* for the above-mentioned reasons).

ii. *Dourdan*, *Sausset2*, and *Vaucresson* displayed correlation coefficients between -0.79 and -0.53 ($p < 10^{-3}$).

iii. Zr was heterogeneously distributed at the surface of the *Greffiere*, *Chanteraines*, and *Compans3* devices – although in the second site a deficit could still be observed near the road pavement –, as a result of which no particular tendency could be noticed in relation to metals.

Figure 3 – Spatial distribution of zinc and zirconium [mg/kg DM] in the surface soil of the study sites *Sausset2*, *Vitry*, and *Alfortville* (plan view). The x- and y-coordinates are given in meters. The arrows indicate the water inflow.

Figure 4 – Spatial distribution of zinc and zirconium [mg/kg DM] in the surface soil and along four cross-sections of the filter strip *Compans2*.

3.2 Zr levels in soil and raw sediment

Zr content was fairly consistent between sites in samples of road-deposited sediment, ranging from 175 to 214 mg/kg DM (Table 2), in accordance with the previous observations of Apeagyei *et al.* (2011). Conversely, the contents found in the reference zone were site-specific, but always greater than in sediment. These values were coherent with the reported levels in soils from the Paris area (Salminen, 2005) albeit slightly higher on average. The *Compans3* swale was the only site where the difference between soil and sediment was < 50 mg/kg DM. In all sites except *Greffiere*, *Chanteraines*, and *Compans3*, the values measured in raw sediment and in non-contaminated soil constituted the two bounds of Zr contents at the surface of the infiltration facilities.

Table 2 – Zr contents in the collected sediment samples and in the reference zone of the study sites. Comparison with literature data for road dust and worldwide soils.
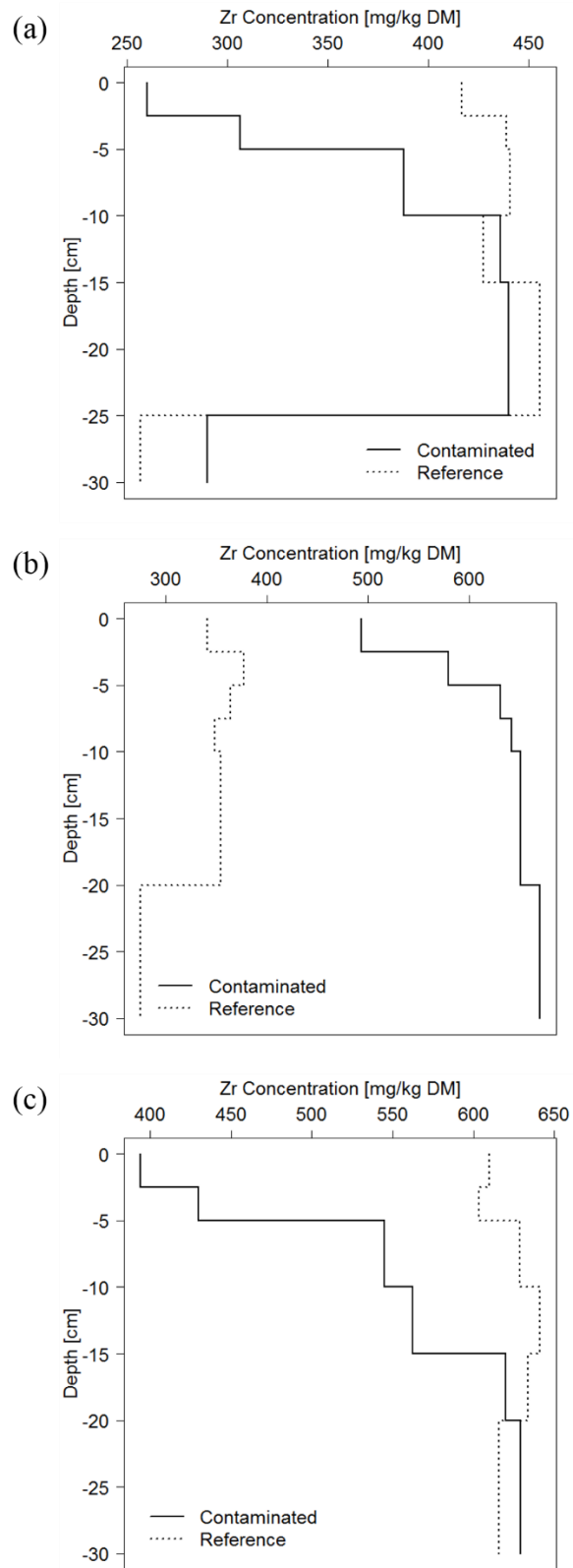
Site	$Zr_{sediment}$ [mg/kg DM]	$Zr_{reference}$ [mg/kg DM]
Dourdan	175	420
Greffiere	214	280
Alfortville	Not sampled[‡]	418
Sausset1	Not sampled	626
Sausset2	Not sampled	501
Chanteraines	178	340
Vitry	209	650
Vaucresson	195	720
Compans1	201	370
Compans2	190	695
Compans3	203	241
Urban road dust (Apeagyei *et al.*, 2011)	180 ± 52 (N = 41)	
Soils from the Paris area (Salminen, 2005)		406 ± 137 (N = 21)
Worldwide soils (Kabata-Pendias, 2011)		200-850
Worldwide soils (Pais and Jones, 1983)		60-2000
American soils (Coughtrey and Thorne, 1983)		70-890

[‡]Sediment deposits could not be found in the immediate vicinity of the sites *Alfortville* and *Sausset*.

3.3 Vertical distribution of Zr

In *Compans1* and *2*, the cross-sections showed that Zr deficit was globally restricted to the upper 5 centimeters alongside the road; the rest of the filter strips displayed almost uniform contents (Figure 4). In the most contaminated zone of the other facilities, Zr content generally tended to increase with depth – which, as for the cartographies, was the opposite trend compared to metals (Tedoldi *et al.*, 2017b). In comparison with the reference profiles, which showed little variability, Zr deficit in the contaminated zone

was visible up to a depth of 5 to 15 cm (Figure 5). In *Alfortville*, the transition between the surface soil and the above-mentioned clay horizon caused a sharp decrease in the measured values (Figure 5a).

Figure 5 – Vertical distribution of the Zr contents [mg/kg DM], in the most and the least contaminated zones of the study sites (a) *Alfortville*, (b) *Chanteraines*, and (c) *Vitry*.

The observations were somewhat different in *Chanteraines*, where the contents measured in the contaminated zone increased with increasing depth, but were significantly higher than in the reference zone (Figure 5b). In *Greffiere* and *Compans3*, similar to what was found at the surface, Zr contents did not show any particular trend with depth and fell in a relatively narrow range of values (225-330 and 185-310 mg/kg DM, respectively).

4. DISCUSSION

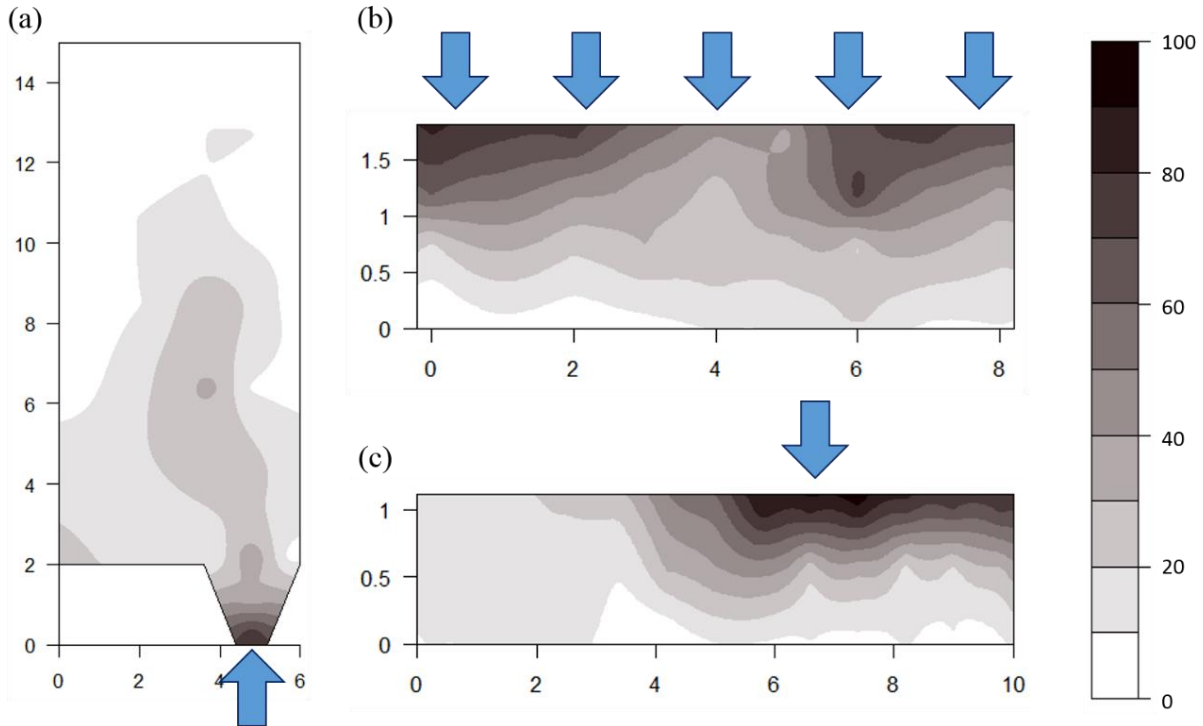### 4.1 Quantification of the sediment fraction

Both horizontally and vertically, a depletion of zirconium (with respect to the site-specific reference values) has been noticed near the inflow zone. Yet, because of its very low mobility in soil, Zr is not likely to have been lixiviated from the upper horizons by the infiltrating water. Hence, the present observations may be explained by the fact that the collected samples were actually a mixture of original soil and other material(s) with different elemental compositions and lower contents of zirconium, resulting in a "dilution" effect in the solid phase. These materials may consist of (*i*) accumulated sediment and/or (*ii*) humus, both of which are likely to be preferentially found near the inflow zone of the devices – vegetation growth was observed to be fostered in the most frequently flooded area, resulting in higher volatile contents (El-Mufleh *et al.*, 2014; Tedoldi *et al.*, 2017a). The typically increasing Zr profiles (*i.e.* decreasing "dilution") with increasing depth over 5-15 cm are also consistent with this interpretation, because of (*i*) filtration processes in the soil matrix, and (*ii*) formation of soil organic matter from the surface litter.

So as to isolate the contribution of sediment accumulation versus organic matter production, Zr contents in every collected sample were expressed per kilogram of *mineral matter* (MM) rather than per kilogram of *dry matter*, knowing the volatile matter content of each sample. This approach relies on the assumption that Zr content in the organic fraction is negligible with respect to the mineral fraction, which seems accurate given its lithogenic sources and low availability to plants (Shahid *et al.*, 2013); for instance, Kabata-Pendias (2011) reported very low Zr contents in histosols, which essentially consist of organic materials (~30 mg/kg DM). Therefore, the "corrected" contents C^*, which are assumed to reflect only the mixture of soil and sediment, may be written as:

$$C^* = f C^*_{\text{sediment}} + (1 - f) C^*_{\text{reference}} \tag{1}$$

where C^*_{sediment} and $C^*_{\text{reference}}$ are the Zr contents in the mineral fraction of raw sediment, and reference soil, respectively [mg/kg MM], and f is the mass fraction of sediment in the sample [-]. In case raw sediment could not be sampled in the immediate vicinity of the infiltration systems (*Alfortville*, *Sausset*), the retained value for C^*_{sediment} was the average of the measurements in sediment samples across all sites (210 mg/kg MM). Eventually, in all facilities except *Greffiere*, *Chanteraines*, and *Compans3*, the spatial distribution of $C^*(x, y)$ in the surface soil enabled the determination of the coefficient $f(x, y)$; in other words, the importance of sediment accumulation could be spatialized (Figure 6). Logically, f was higher in

the inflow zone of each investigated system (up to 80% in *Vitry* and *Vaucresson*, and almost 100% in *Compans1* and *2*), demonstrating that particle settling predominantly occurs in a relatively narrow area.

Figure 6 – Spatial distribution of the sediment fraction f [%] at the surface of the study sites (a) *Sausset1*, (b) *Vitry*, and (c) *Vaucresson* (plan view). The arrows indicate the water inflow.

As regards the "exception sites" with dissimilar behaviors, it should be underlined that the *Greffiere* facility was implemented in a residential area with *a priori* low suspended solid loads, while the heterogeneity observed in the *Chanteraines* and *Compans3* swales may be attributed to an uneven mixture of the soil material during their construction. In the former case, this would also explain the dissimilarity in Zr profiles between the contaminated and the reference zones (Figure 5b), which was also visible with the distribution of other metals or pedological parameters such as cation exchange capacity or carbonates (Tedoldi *et al*., 2017b). In the latter case, not only was the differential between the sediment and soil relatively small, but also the operating time of the system (1 year) was probably insufficient to observe a significant sediment buildup in the swale.

By applying equation (1) to Zr profiles, the fraction f could also be determined and plotted as a function of depth. $C^*_{\text{reference}}$ was taken as the mean value of the corrected contents over 0-30 cm depth in the reference zone, excluding the deepest sample in *Alfortville*, as it corresponded to a different horizon of soil. However, the retained value for $C^*_{\text{reference}}$ in *Chanteraines* was the content in the deepest sample from the most contaminated zone (700 mg/kg MM) because of the differences in elemental composition between the two parts of the swale. Although the results from *Compans1* and *2* suggested a "cake filtration" effect near the pavement (Figure 4), the profiles obtained in the other sites (except *Greffiere* and *Compans3*) depicted the accumulation of suspended solids *within* the soil matrix and thus proved the occurrence of bed filtration

over 5 to 15 cm, in addition to sediment accumulation at the surface (Figure 7). The calculations showed that there were almost 20% of sediments in the 5-10 cm segment of *Alfortville* and *Vitry*, indicating a state of advanced clogging, contrary to the other sites. The penetration of such quantities of sediments at this depth is plausible, considering the age of the devices, the significant suspended solid production from their catchments (industrial areas with high truck traffic), and the renewal of the soil porosity near the surface due to vegetation roots and biological activity, as described by Paus *et al.* (2013) and Cannavo *et al.* (2018).

4.2 Calibration of a filtration model

Theoretical background. A series of models with contrasting complexity are available to describe the attachment and transfer of suspended solids within a porous material, using either a microscopic or a macroscopic approach (Logan, 2001; Li and Davis, 2008b). Among the second category, the simplest one is usually referred to as Iwasaki's model (Iwasaki, 1937), which consists of a set of two equations:

$$q \frac{\partial C_p}{\partial z} + \frac{\partial \sigma_p}{\partial t} = 0 \tag{2}$$

$$\frac{\partial C_p}{\partial z} = -\lambda C_p \tag{3}$$

where C_p is the mass concentration of particles in the percolating water [M.L^{-3}], q is the Darcy velocity [L.T^{-1}], σ_p is the mass of deposited solids per unit bed volume [M.L^{-3}], z is the vertical coordinate [L] (increasing downwards), and λ is called the *filter coefficient* [L^{-1}]. Equation (2) is a simplified form of the continuity equation, which expresses the mass balance between the solids removed from suspension and those deposited in the pores of the media. In equation (3), a high value of λ indicates a good efficiency of the media for particle retention, resulting in an important accumulation near the surface. Some studies introduced an empirical relationship $\lambda = f(\sigma_p)$ to represent the effects of progressive soil clogging (Logan, 2001). In case λ is assumed constant, this parameter is often estimated experimentally from the ratio between influent and effluent concentrations, considering either soil columns, or *in-situ* bioretention systems (Li and Davis, 2008a,b). Yet, it is onerous and not always possible to collect the effluent water, especially in infiltration devices which are not equipped with an underdrain. Although several authors proposed analytical expressions for the parameter λ, *e.g.* as a function of the bed porosity and size of the "collectors", they still introduced empirical parameters such as the "attachment efficiency" or the "collision efficiency" of the particles (Yao *et al.*, 1971), which are not immediately available.

As the present approach directly provides the vertical distribution of filtered solids in the soil, it may be valuably used to calibrate such models. The mass content of retained particles σ_m (*i.e.* expressed per unit bed *mass*) is linked to the variable σ_p *via* the relationship $\sigma_p = \rho \sigma_m$, where ρ is the bulk density of the porous media [M.L^{-3}] – so combining equations 2 and 3 yields:

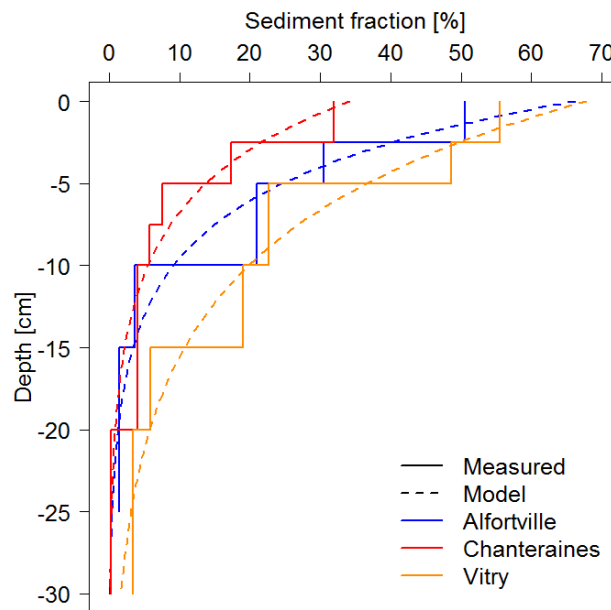$$\frac{\partial \sigma_m}{\partial t} = \frac{\lambda}{\rho} q C_p \tag{4}$$

Time integration of equation (4) finally leads to:

$$\sigma_m(z,t) = \sigma_0(z) + \frac{\lambda}{\rho} \int_0^t q(z,\tau)\, C_p(z,\tau)\, d\tau \qquad (5)$$

If the soil is assumed to be initially clean ($\sigma_0 = 0$), and q is assumed to be uniform on average over the considered soil depth (30 cm) – which seems acceptable for the most contaminated zone, as it corresponds to the most frequently flooded area where the infiltration fluxes are concentrated – then the variable σ_m theoretically follows the same spatial variations as C_p, *i.e.* the exponential distribution imposed by equation (3).

Application to the data. A linear regression was carried out on the log-transformed fraction f as a function of z, assigning to each vertical segment its average depth. The satisfactory adjustment provided by the linear model in *Alfortville*, *Sausset1*, *Sausset2*, *Chanteraines*, and *Vitry* ($R^2 > 0.85$) confirmed the validity of these theoretical developments. The filter coefficient λ was estimated as the slope of the regression and ranged from 0.12 cm^{-1} (in *Vitry*) to 0.20 cm^{-1} (in *Alfortville*). These values are consistent with the data reported by Leclerc (1998), which varied between 0.08 and 0.50 cm^{-1}. They are slightly lower than the experimental measurements carried out by Li and Davis (2008b) in soil columns, which fell between 0.34 and 0.55 cm^{-1}, but higher than the same authors' *in-situ* estimations on a bioretention cell (0.01-0.06 cm^{-1}) (Li and Davis, 2008a). These differences can be explained by the fact that (*i*) for column experiments, the soil material is generally homogenized and uniformly packed, so the filtration performance may be expected to be higher than for a real system, (*ii*) the particle size and pore size distributions are likely to be different between the presently assessed devices and the above-mentioned bioretention cell (made of 50% sand, 30% topsoil, and 20% mulch), and (*iii*) when studying a real system, soil particles may be lixiviated during water infiltration, thus leading to an underestimation of the filter coefficient.

Figure 7 – Measured (solid lines) and calibrated (dotes lines) sediment fraction f [%] as a function of depth, in the study sites *Alfortville*, *Chanteraines*, and *Vitry*.

4.3 Uncertainties, applicability and limits of the method

The objective of this section is to assess the robustness of the results with respect to the uncertainties on the Zr contents, which can be classified into four components. (*i*) Analytical uncertainties are related to the repeatability of the XRF measurements, which was characterized by an average coefficient of variation of 3% (calculated from the 5 to 6 analyses carried out on different subsamples) and modelled with a normal distribution centered about the mean value for each sample. (*ii*) Zr contents in the reference zone were never exactly uniform, as a result of which the retained values for $C^*_{\text{reference}}$ may be somewhat biased. The "local", site-specific variability of reference contents was represented with a normal distribution for each device. (*iii*) In spite of a relative inter-site stability of the Zr content in raw sediment, some uncertainty is associated with the estimation of C^*_{sediment} when sediment samples could not be collected on the nearby pavement. Between sites, values ranged from 195 to 238 mg/kg MM, and this interval extended to 187-247 mg/kg MM when accounting for the analytical uncertainties. Accordingly, the uncertainty about C^*_{sediment} in *Alfortville* and *Sausset* was represented with a uniform distribution. (*iv*) Finally, it should be mentioned that the particles which are most likely to settle on the road are the coarser ones, and thus may be non-representative of the entire distribution of suspended solids in runoff (*e.g.* with lower organic matter contents), but this point was not accounted for in the subsequent calculations.

These uncertainties imply the existence of a minimal degree of dilution below which sediment accumulation cannot be considered as significant (*i.e.* the hypothesis that $f = 0$ cannot be rejected). Evidently, the greater the difference between $C^*_{\text{reference}}$ and C^*_{sediment}, the lower is the "limit of quantification" of the sediment fraction, which was found to lie between 7 and 11% (w/w) for *Dourdan*, *Alfortville*, *Sausset1* and *2*, *Chanteraines*, *Vitry*, *Vaucresson*, and *Compans2*. Conversely, this value was higher in *Compans1* (~25%) and *Greffiere* (~75%), while it was almost 100% in *Compans3* due to notably low Zr contents in the filter media.

Finally, a stochastic approach was carried out in order to assess the impact of these uncertainties on the calculated filter coefficient. The estimation procedure was repeated 10 000 times for each site, with C^*_{sediment} and $C^*_{\text{reference}}$ randomly sampled from their respective distributions, leading to statistical data for the parameter λ. In the three examples displayed in Figure 7, the associated 95% confidence intervals were 0.11-0.30 cm^{-1} for *Alfortville*, 0.08-0.34 cm^{-1} for *Chanteraines*, and 0.08-0.20 cm^{-1} for *Vitry*. Therefore, although the proposed method appears to be somewhat sensitive to the estimated zirconium content in both raw sediment and non-contaminated soil, the resulting uncertainty on the parameter λ is quite comparable to the other experimental methods, and one of its major improvements lies in the fact that the procedure does not require sampling soil water.

The study sites *Greffiere* and *Compans3*, along with *Chanteraines* for the cartography stage, provided three examples where the proposed methodology is not applicable:

    i.   the geochemical background of Zr is close to the content in raw sediment;

ii.   sediment accumulation is not sufficient to discriminate between Zr deficit and the natural variations of this element – either due to a short operating time or to low suspended solid loads from the watershed;

iii. the mixing of the soil material before backfilling the infiltration devices is uneven.

Regarding the first point, the variability of Zr levels in worldwide soils (as reported in Table 2) suggests that this method may be successfully implemented in many contexts beyond the Paris region, excluding the zones with Zr contents close to the "critical" value of 200 mg/kg DM – or perhaps biofiltration systems composed of an engineered filter media, the composition of which may be different from natural soils. In such cases, the present approach is certainly transposable with another tracer among the usual geochemical invariants (*e.g.* titanium or aluminum), which should be further investigated and may enable the validation of the results obtained with zirconium.

5. CONCLUSIONS AND PERSPECTIVES

The present work validated the use of zirconium as a tracer of sediment accumulation in soil-based Sustainable Urban Drainage Systems. Zr and metal levels were analyzed in road-deposited sediment as well as more than 500 surface soil samples and 175 samples along vertical profiles from 11 study sites. Zr content in "raw" sediment was found to be significantly lower than in non-contaminated soil, with a noteworthy inter-site stability. In most devices, Zr showed "mirror" distributions with respect to metals, *i.e.* a deficit of Zr could be noticed horizontally and vertically in the most contaminated zone. Since Zr is unlikely to be leached or taken up by plants because of its physicochemical properties, this observation was interpreted as the result of a "dilution" in the solid phase due to sediment accumulation. The "dilution ratio" enabled the calculation of the sediment fraction, the spatial variability of which provided evidence for the joint occurrence of particle settling over a limited part of the surface and bed filtration within the soil matrix.

Several sources of uncertainty, including the repeatability of the analyses and the natural variability of Zr in soil, resulted in a site-specific "limit of quantification" for the sediment fraction, which was generally found to be around 10% (w/w), except when the geochemical background was close to the Zr level in sediment. Hence the proposed approach appeared to be reasonably precise and appropriate for many geological contexts beyond the present experimental area. These findings were used to calibrate a simple, one-dimensional filtration model. In most study sites, the measured profiles were consistent with the exponential distribution derived from Iwasaki's equation, and the filter coefficient could be calculated with a controlled confidence interval. The accuracy of the measurement was comparable with other methods available in the literature, and the approach presented the considerable advantage that it did not require sampling soil water. Another perspective of this work may be to further investigate the occurrence of soil clogging in infiltration

systems, so as to better understand the antagonistic effects of particle accumulation versus biological renewal of the soil porosity.

ACKNOWLEDGEMENTS

REFERENCES

Apeagyei, E., Bank, M. S., Spengler, J. D. Distribution of heavy metals in road dust along an urban-rural gradient in Massachusetts. *Atmospheric Environment,* **2011**, 45(13), 2310-2323.

Cannavo, P., Coulon, A., Charpentier, S., Béchet, B., Vidal-Beaudet, L. Water balance prediction in stormwater infiltration basins using 2-D modeling: An application to evaluate the clogging process. *International Journal of Sediment Research*, **2018**, *in press*.

Coughtrey, P.-J., Thorne, M.-C. *Radionuclide distribution and transport in terrestrial and aquatic ecosystems : a critical review of data. Volume one.* A. A. Balkema, Rotterdam, **1983**.

Clark, S. E., Pitt, R. Targeting treatment technologies to address specific stormwater pollutants and numeric discharge limits. *Water Research*, **2012**, 46, 6715-6730.

Dierkes, C., Lucke, T., Helmreich, B. General technical approvals for decentralised Sustainable Urban Drainage Systems (SUDS) – The current situation in Germany. *Sustainability,* **2015**, 7(3), 3031-3051.

Egli, M., Fitze, P. Formulation of pedologic mass balance based on immobile elements: a revision. *Soil Science,* **2000**, 165(5), 437-443.

El-Mufleh, A., Béchet, B., Ruban, V., Legret, M., Clozel, B., Barraud, S., Gonzalez-Merchan, C., Bedell, J.-P., Delolme, C. Review on physical and chemical characterizations of contaminated sediments from urban stormwater infiltration basins within the framework of the French observatory for urban hydrology (SOERE URBIS). *Environmental Science and Pollution Research,* **2014**, 21(8), 5329-5346.

Erickson, A. J., Weiss, P. T., Gulliver, J. S. *Optimizing stormwater treatment practices: a handbook of assessment and maintenance.* Springer, New York, **2013**.

Flanagan, K., Tedoldi, D., Branchu, P., Gromaire, M.-C. Caractérisation du fonctionnement d'un ouvrage de gestion à la source du ruissellement de voirie : approche par modélisation hydrologique et par cartographie de la contamination du sol. *La Houille blanche,* **2017**, 3, 5-13.

Fletcher, T. D., Andrieu, H., Hamel, P. Understanding, management and modelling of urban hydrology and its consequences for receiving waters; a state of the art review. *Advances in Water Resources*, **2013**, 51, 261–279.

Fletcher, T. D., Shuster, W., Hunt, W. F., Ashley, R., Butler, D., Arthur, S., Trowsdale, S., Barraud, S., Semadeni-Davies, A., Bertrand-Krajewski, J.-L., Mikkelsen, P. S., Rivard, G., Uhl, M., Dagenais, D.,

Viklander, M. SUDS, LID, BMPs, WSUD and more – The evolution and application of terminology surrounding urban drainage. *Urban Water Journal*, **2015**, 12(7), 525-542.

Göbel, P., Dierkes, C., Coldewey, W. G. Storm water runoff concentration matrix for urban areas. *Journal of Contaminant Hydrology*, **2007**, 91(1-2), 26-42.

Hatt, B. E., Fletcher, T. D., Walsh, C. J., Taylor, S. L. The influence of urban density and drainage infrastructure on the concentrations and loads of pollutants in small streams. *Environmental Management*, **2004**, 34(1), 112-124.

Huber, M., Welker, A., Helmreich, B. Critical review of heavy metal pollution of traffic area runoff: Occurrence, influencing factors, and partitioning. *Science of the Total Environment,* **2016**, 541, 895-919.

ISO 11464. *Soil quality – Pretreatment of samples for physico-chemical analysis.* International Organization for Standardization, Geneva, **2006**.

Iwasaki, T. Some notes on sand filtration. *American Water Works Association,* **1937**, 29, 1591-1602.

Kabata-Pendias, A. *Trace Elements in Soils and Plants, Fourth edition.* CRC Press, Boca Raton, **2011**.

Kluge, B., Wessolek, G. Heavy metal pattern and solute concentration in soils along the oldest highway of the world – the AVUS Autobahn. *Environmental Monitoring and Assessment,* **2012**, 184(11), 6469-6481.

Leclerc, D. Filtration en profondeur – Aspects théoriques. *Techniques de l'ingénieur*, **1998**, 1-8.

Li, H., Davis, A. P. Heavy metal capture and accumulation in bioretention media. *Environmental Science and Technology,* **2008a**, 42(14), 5247-5253.

Li, H., Davis, A. P. Urban particle capture in bioretention media. II: Theory and model development. *Journal of Environmental Engineering,* **2008b**, 134(6), 419-432.

Logan, J. D. *Transport Modeling in Hydrogeochemical Systems.* Springer, New York, **2001**.

McGrane, S. J. Impacts of urbanisation on hydrological and water quality dynamics, and urban water management: a review. *Hydrological Sciences Journal*, 2016, 61(13), 2295-2311.

Miller, J. D.; Kim, H.; Kjeldsen, T. R.; Packman, J.; Grebby, S. Assessing the impact of urbanization on storm runoff in a peri-urban catchment using historical change in impervious cover. *Journal of Hydrology,* **2014**, 515, 59-70.

Mohiuddin, K. M., Zakir, H. M., Otomo, K., Sharmin, S., Shikazono, N. Geochemical distribution of trace metal pollutants in water and sediments of downstream of an urban river. *International Journal of Environmental Science and Technology,* **2010**, 7(1), 17-28.

Napier, F., Jefferies, C., Heal, K. V., Fogg, P., d'Arcy, B. J., Clarke, R. Evidence of traffic-related pollutant control in soil-based Sustainable Urban Drainage Systems (SUDS). *Water Science and Technology,* **2009**, 60(1), 221-230.

Pais, I., Jones, J. B. *The Handbook of Trace Elements*, CRC Press, Boca Raton, **1983**.

Paus, K. H., Morgan, J., Gulliver, J. S., Leiknes, T., Hozalski, R. M. Assessment of the hydraulic and toxic metal removal capacies of bioretention cells after 2 to 8 years of service. *Water, Air and Soil Pollution,* **2013**, 225(1), 1803.

Salminen, R. (Chief ed.). *Geochemical Atlas of Europe. Part 1 – Background Information, Methodology, and Maps*. Geological Survey of Finland, Espoo, **2005**.

Schulz, R. K. Soil chemistry of radionuclides. *Health Physics,* **1965**, 11(12), 1317-1324.

Shahid, M., Ferrand, E., Schreck, E., Dumat, C. Behavior and impact of zirconium in the Soil-Plant System: Plant uptake and phytotoxicity. *Reviews of Environmental Contamination and Toxicology,* **2013**, 221, 107-127.

Sposito, G. *The chemistry of soils, second edition.* Oxford University Press, Oxford, **2008**.

Stockmann, U., Cattle, S. R., Minasny, B., McBratney, A. B. Utilizing portable X-ray fluorescence spectrometry for in-field investigation of pedogenesis. *Catena*, **2016**, 220-231, 139.

Tedoldi, D., Chebbo, G., Pierlot, D., Kovacs, Y., Gromaire, M.-C. Impact of runoff infiltration on contaminant accumulation and transport in the soil/filter media of Sustainable Urban Drainage Systems: A literature review. *Science of the Total Environment,* **2016**, 569-570, 904-926.

Tedoldi, D., Chebbo, G., Pierlot, D., Branchu, P., Kovacs, Y., Gromaire, M.-C. Spatial distribution of heavy metals in the surface soil of source-control stormwater infiltration devices – Inter-site comparison. *Science of the Total Environment,* **2017a**, 579, 881-892.

Tedoldi, D., Chebbo, G., Pierlot, D., Kovacs, Y., Gromaire, M.-C. Assessment of metal and PAH profiles in SUDS soil based on an improved experimental procedure. *Journal of Environmental Management,* **2017b**, 202, 151-166.

Yao, K.-M., Habibian, M. T., O'Melia, C. R. Water and waste water filtration: Concepts and applications. *Environmental Science and Technology,* **1971**, 5(11), 1105-1112.